

# Probing Hydrophobic Nanocavities in Chemical and Biological Systems with a Fluorescent Proton-Transfer Dye

Irene García-Ochoa,<sup>[a]</sup> María-Ángeles Díez López,<sup>[a]</sup> Montserrat H. Viñas,<sup>[b]</sup> Lucía Santos,<sup>[c]</sup> Ernesto Martínez Atáz,<sup>[c]</sup> Francisco Amat-Guerri,<sup>[d]</sup> and Abderrazzak Douhal\*<sup>[a]</sup>

**Abstract:** A new and sensitive molecular probe, namely, 2-(2'-hydroxyphenyl)-4-methyloxazole (HPMO), for exploring nanocavities in chemical and biological systems is presented. The incorporation of HP MO into hydrophobic cavities in aqueous medium involves rupture of its intermolecular hydrogen bond to water and formation of an intramolecular hydrogen bond in the sequestered molecule. Upon UV excita-

tion (280–330 nm) of this entity, a fast intramolecular proton-transfer reaction of the excited state produces a phototautomer, the fluorescence of which ( $\lambda_{\text{max}} = 450\text{--}470\text{ nm}$ ) shows a largely Stokes-shifted band. Because of the existence of a twisting motion around

**Keywords:** dyes • fluorescence spectroscopy • hydrogen bonds • inclusion compounds • proton transfer

the C2–C1' bond of this phototautomer, the absorption and emission properties of the probe depend on the size of the host cavity. Experiments with cyclodextrins, calix[4]arene, micelles and the human protein serum albumin reveal that the emission of the sequestered phototautomer of HP MO is a simple and efficient tool for detecting and exploring the size of hydrophobic nanocavities.

## Introduction

Molecules that are surrounded by other molecules provide the opportunity to examine solvation,<sup>[1]</sup> desolvation,<sup>[2]</sup> intermediates,<sup>[3]</sup> intermolecular and intramolecular reactions,<sup>[4]</sup> and stereoisomerism.<sup>[5]</sup> Among the simplest and most promising systems are inclusion complexes of dyes and cyclodextrins (CDs),<sup>[6–13]</sup> which allow the effect of confined geometries on the spectroscopy and dynamics of simple and complex reactions to be studied. Recently, such molecular pockets were used to observe a twisting motion in the dynamics of excited-state intramolecular proton-transfer (ESIPT) reactions.<sup>[12, 13]</sup> On the basis of these results, we proposed a novel way to explore the structural dynamics of lipid bilayers<sup>[14]</sup> and to probe nanocavities of chemical media.<sup>[12]</sup>

Here we describe the absorption and emission properties of a dye trapped in the hydrophobic pockets of CDs, *n*-octyl- $\beta$ -D-glucopyranoside micelle, *cyclo*-undecyl-calix[4]resorcinarene (calix[4]arene), and human serum albumin (HSA) protein in water (Scheme 1).

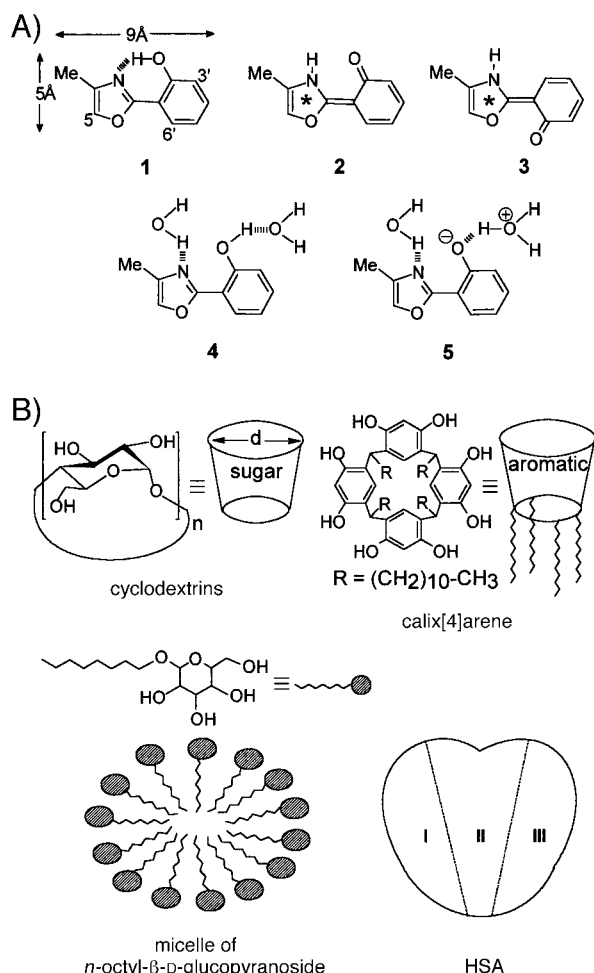
The dye 2-(2'-hydroxyphenyl)-4-methyloxazole (HPMO, **1**)<sup>[15]</sup> is a heterocyclic molecule with an intramolecular hydrogen bond and the possibility of twisting around the C2–C1' bond (Scheme 1A). When irradiated with UV light (240–340 nm), **1** shows an absorption maximum at about 320 nm and a fluorescence band with a maximum at around 470 nm (Stokes shift ca. 10000 cm<sup>-1</sup>). The emission is ascribed to **2** or **3**, depending on the rigidity of the medium.<sup>[13, 15]</sup> Proton transfer in **1** occurs in less than 300 femtoseconds, and the internal rotation about the the C2–C1' bond of excited **2** to yield **3** in fluid media takes place on the picosecond time scale.<sup>[13]</sup> Both times are markedly influenced by confined geometries and, in particular, a noticeable decrease in barrier crossing from **2** to **3** is observed.<sup>[13]</sup> The driving force for proton transfer is provided by simultaneous large changes in the acidity and basicity of the involved groups. The swings in p*K*<sub>a</sub> values arise from a fast electronic redistribution induced by light and a vibrational coherence of the elementary modes that modulate the hydrogen-bond coordinates.<sup>[13–19]</sup> We exploit the hydrophobic/hydrophilic interactions of HP MO with the environment for monitoring the size and/or rigidity of the internal cavity of chemical and biological systems.

[a] Prof. A. Douhal, I. García-Ochoa, M.-A. Díez López  
Departamento de Química Física, Facultad de Ciencias del Medio Ambiente  
Universidad de Castilla-La Mancha  
San Lucas 3, E-45002 Toledo (Spain)  
Fax: (+34) 925-253614  
E-mail: adouhal@qui-to.uclm.es

[b] Prof. M. H. Viñas  
Universidad Politécnica de Madrid, E-28031 Madrid (Spain)

[c] Prof. L. Santos, Prof. E. Martínez Atáz  
Universidad de Castilla-La Mancha, E-13004 Ciudad Real (Spain)

[d] Dr. F. Amat-Guerri  
Instituto de Química Orgánica, CSIC, E-28006 Madrid (Spain)



Scheme 1. A) Molecular structures of the different species of 2-(2'-hydroxyphenyl)-4-methyl-5-oxazolone (HPMO). B) Structures of  $\alpha$ - ( $n=6$ ,  $d=5.7$  Å),  $\beta$ - ( $n=7$ ,  $d=7.8$  Å), and  $\gamma$ -cyclodextrin ( $n=8$ ,  $d=9.5$  Å); cyclo-undecylcalix[4]resorcinarene; *n*-octyl- $\beta$ -D-glucopyranoside micelle; and a schematic illustration of human serum albumin (HSA) protein topology with the domains I, II and III.

**Abstract in Spanish:** *En este trabajo se presenta un nuevo y sensible sensor molecular, 2-(2'-hidroxifenil)-4-metiloxazol (HPMO), útil para el estudio de nanocavidades en sistemas químicos y biológicos. En medio acuoso, HPMP se encuentra formando enlaces de hidrógeno con el agua, pero estos enlaces se rompen cuando el compuesto se incluye en el interior de cavidades hidrofóbicas, formándose entonces un enlace de hidrógeno intramolecular. La fotoexcitación (280–330 nm) de la especie secuestrada produce una rápida transferencia protónica intramolecular en el estado excitado. Como resultado se forma un fototautómero cuya fluorescencia muestra un gran desplazamiento de Stokes (máximo en el entorno 450–470 nm). Debido a que este fototautómero tiende a estabilizarse por giro alrededor del enlace C2–C1', que une los dos anillos de la molécula, los espectros de absorción y de emisión dependen del tamaño de la cavidad del huésped. Los experimentos con ciclodextrinas, calix[4]areno, micelas y la proteína seroalbúmina humana demuestran que la emisión del fototautómero secuestrado es una herramienta simple y eficiente para detectar y sondear el tamaño de las nanocavidades hidrofóbicas en estos sistemas.*

## Results and Discussion

Figure 1 shows UV/Vis absorption and fluorescence spectra of HPMP in water and in 3-methylpentane (3MP). In 3MP, absorption is due to structure **1**, and emission originates from

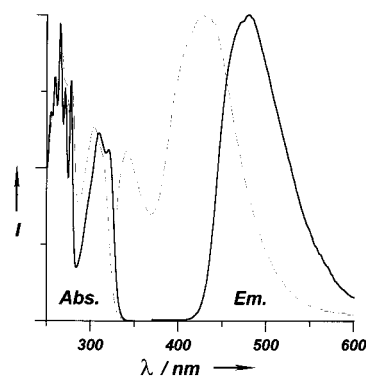


Figure 1. Normalized UV/Vis absorption (Abs.) and emission (Em.,  $\lambda_{\text{ex}} = 320$  nm) spectra of  $10^{-6}$  M HPMP in 3-methylpentane (—) and in water (---) (pH 6).  $I$  = intensity.

**3** (Scheme 1A).<sup>[13]</sup> Evidence for emission from **3** was deduced from femtosecond experiments in this solvent and in caging media in which formation of **3** is prevented.<sup>[13]</sup> In addition, ab initio calculations indicate the possible formation of **3** as a local minimum on the potential-energy surface of the excited state.<sup>[15]</sup> In water, absorption and emission spectra of HPMP correspond to solvated structures **4** ( $\lambda_{\text{max}} \approx 314, 350$  nm). In addition to the emission at 350 nm, excited **4** undergoes an intermolecular proton-transfer reaction with water that leads to the phenolate-type structure **5**, which has a stronger emission band at 425 nm. These assignments are based on the behavior of HPMP in acidic, neutral, and alkaline aqueous solutions, in which the molecular structure of the absorbing and emitting species can be controlled by adjusting the pH of the medium. The fluorescence decay of **5** fits to a biexponential function with time constants of 0.22 and 2.64 ns. The biexponential behavior might be a consequence of a fast twisting motion (in plane and out of plane) of the phenolate moiety that leads to different twisted conformers.

Upon addition of  $\beta$ -CD (largest diameter ca. 7.8 Å),<sup>[4, 6]</sup> to an aqueous solution of HPMP, the absorption band (314 nm) is red-shifted to 322 nm (Figure 2A), and the emission band now has a maximum at 465 nm (Figure 2B). The emission intensity at 350 and 425 nm decreases. The band at 465 nm is assigned to **2** confined in the cavity of CD. The fluorescence decay at 480 nm, measured with a nanosecond apparatus, is biexponential with time constants of 0.5 (68%) and 3.2 ns (32%). On the basis of the very similar absorption and emission spectra in water in the absence and presence of the linear oligosaccharide maltoheptose (data not shown), we conclude that the changes observed with  $\beta$ -CD are due to encapsulation of HPMP.

To gain information on the inclusion mode, we recorded <sup>1</sup>H NMR spectra of HPMP in D<sub>2</sub>O in the absence and presence of  $\beta$ -CD (Figure 3A). The protons at positions 5 and 6' and those of the 4-methyl group of HPMP undergo the

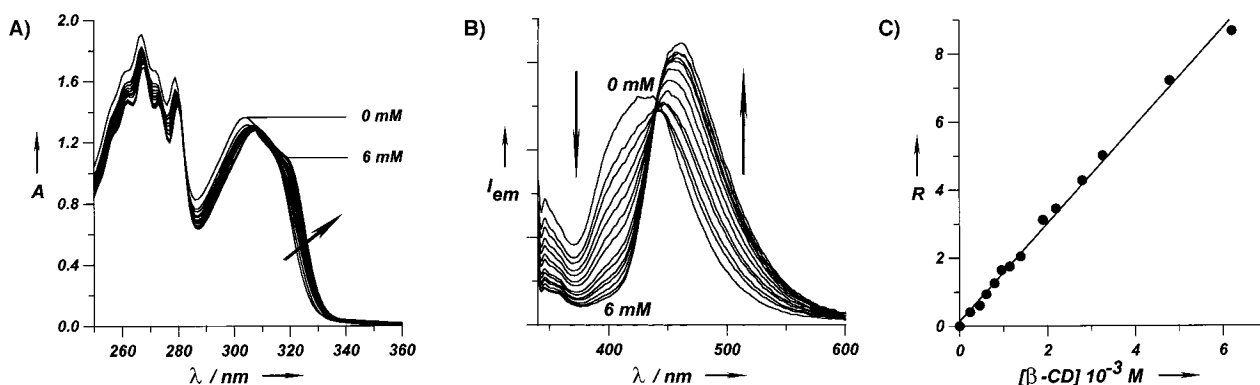


Figure 2. UV/Vis absorption (A) and emission (B) spectra ( $\lambda_{\text{ex}} = 320$  nm) of HP MO in water ( $\beta$ -CD) and upon addition of  $\beta$ -CD. C) Plot of the changes in the fluorescence intensity ratio  $R$  (intensity at 480 nm/intensity at 400 nm) versus  $\beta$ -CD concentration. The inclusion equilibrium constant for the complex HP MO: $\beta$ -CD is the slope of the line when  $[\text{HP MO}] \ll [\beta\text{-CD}]$ .  $A$  = absorbance,  $I_{\text{em}}$  = emission intensity.

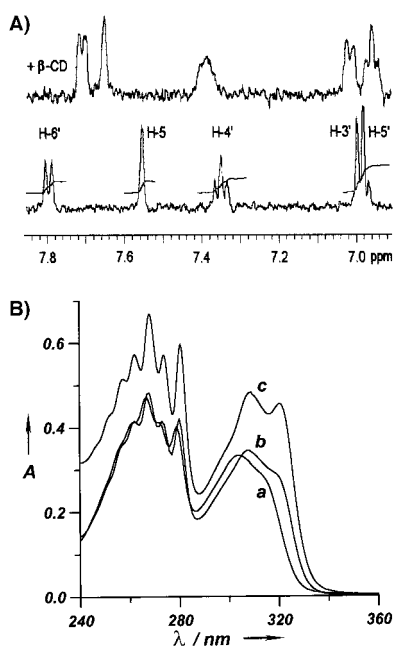
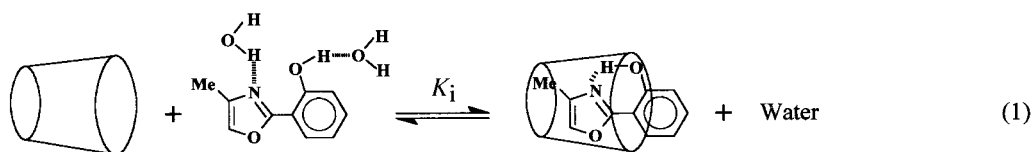


Figure 3. A) Aromatic region of comparative  $^1\text{H}$  NMR spectra (500 MHz,  $\text{D}_2\text{O}$ , 303 K) of  $10^{-3}\text{M}$  HP MO in the absence (bottom) and presence (top) of  $10^{-2}\text{M}$   $\beta$ -CD. B) UV absorption spectra of HP MO in water (a), water containing  $\beta$ -CD (b), and dioxane (c).

largest shifts upon inclusion ( $\Delta\delta = +0.11$ ,  $-0.08$ , and  $+0.07$ , respectively). This suggests that the oxazole component of the guest is sequestered by the CD cavity. If the phenol moiety were sequestered, the shifts for H3', H4', and H5' would be higher. Thus, the reaction leading to the 1:1 complex can be represented by Equation (1). The inclusion equilibrium constant  $K_i$  at 300 K was derived from the changes in emission intensities at 400 and 480 nm ( $K_i = 1400 \pm 50\text{M}^{-1}$ ) with increasing concentration of  $\beta$ -CD (Figure 2C). The conformation of the ground-state species encapsulated by  $\beta$ -CD must be similar to that of **1**, which is the major structure of HP MO in dioxane (Figure 3B).



The steady-state anisotropy  $\langle r \rangle$  (see Experimental Section) of the emission band at 465 nm for the  $\beta$ -CD complex is  $0.115 \pm 0.006$ . This indicates some reorientation of the excited phototautomer, in agreement with the relation between the size of the guest (HP MO, length ca. 9 Å, diameter ca. 5 Å) and the diameter of the cavity of the host ( $\beta$ -CD, largest diameter ca. 7.8 Å) (Scheme 1). On the basis of these results, as well as ab initio calculations<sup>[15]</sup> and femtosecond experiments,<sup>[13]</sup> we examined the spectral properties of aqueous solutions of HP MO sequestered by  $\alpha$ - and  $\gamma$ -CD, which have largest diameters of 5.7 and 9.5 Å, respectively.<sup>[4,6]</sup> The emission maximum of the band of the phototautomer which results from ES IPT reaction of HP MO entrapped by  $\alpha$ -,  $\beta$ -, and  $\gamma$ -CD appears at 450, 465 and 470 nm, respectively (Figure 4A). Those of excitation bands of these emissions are located at 317, 322, and 325 nm, respectively.

The red shift of the absorption maximum of the inclusion complex when the diameter of the CD cavity is increased indicates rotation about the C2–C1' bond of the guest upon inclusion. As a result of encapsulation, formation of an intramolecular  $\text{OH} \cdots \text{N}$  bond leads to a confined geometry **1**:CD complex. A blue shift indicates a weaker conjugation between the  $\pi$  orbitals of the aromatic moieties of the guest owing to nonplanarity. Due to steric hindrance in  $\alpha$ -CD for instance, the guest cannot relax to a more highly conjugated geometry. In contrast, the larger space offered by  $\gamma$ -CD allows twisting around C2–C1' to give a more planar geometry.

A similar trend is observed in the emission spectrum upon UV irradiation of the confined-geometry complex. The relaxation route of the excited tautomer depends on the diameter of the cyclodextrin. Emission can occur from **2** or **3**, depending on the degrees of freedom (space) provided by the CD cavity. In  $\alpha$ -CD, the emission originates from **2**, while in  $\gamma$ -CD it is mainly due to **3**. If emission in these pockets occurs from a single conformer and is independent of the host cavity, a quenching mechanism that leads to nonradiative states cannot explain the shift of the emission band on changing the

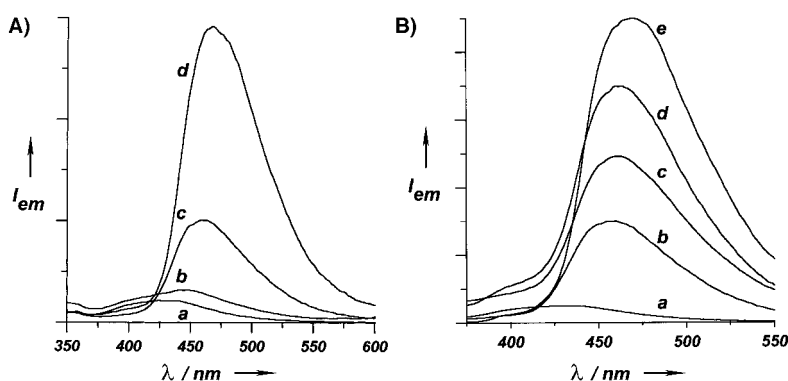


Figure 4. A) Emission ( $\lambda_{ex} = 320$  nm) spectra of HPMO in water (a), and in water containing 7 mM  $\alpha$ - (b),  $\beta$ - (c), or  $\gamma$ -cyclodextrins (d). B) Emission spectra of HPMO in water (a); in presence of 30 mM *n*-octyl- $\beta$ -D-glucopyranoside micelle (b), 1.3 mM *cyclo*-undecylcalix[4]resorcinarene (c), and 3.4  $\mu$ M HSA (d); and emission in pure triacetin (e). For clarity, the intensities of (c) and (d) are magnified by a factor of three.

diameter of the cavity. We suggest that the observed spectral shift is due to rotational motion of the (sequestered) phototautomer which results from ESIPT reaction in the guest **1**. These conclusions agree with the results of *ab initio* calculations<sup>[15]</sup> and femtosecond experiments.<sup>[13]</sup> In addition, jet-cooled molecular beam experiments on a similar molecule, namely, 2-(2'-hydroxyphenyl)-5-phenyloxazole, indicated the involvement of in-plane and out-of-plane motions of the phenol moiety in the proton-transfer process,<sup>[20]</sup> in agreement with frequency analysis of the theoretical calculations.<sup>[15]</sup> It is noteworthy that by caging this type of dye, one can control the dynamics (time domain) and spectroscopy (frequency domain) of ESIPT reaction.<sup>[13-18]</sup>

One of our goals was to show a simple and efficient switch from hydrophilic to hydrophobic interactions, so that coupling of the proton transfer and the twisting motion can be used for exploring hydrophobic nanocavities in chemical and biological systems. To this end, we recorded the emission spectra of HPMO in aqueous solutions of *n*-octyl- $\beta$ -D-glucopyranoside micelles, calix[4]arene, and HSA (Scheme 1B). For comparison, we recorded the emission spectrum in triacetin, a weak hydrogen-bonding, but viscous environment ( $\eta = 22$  cP at 20 °C). As Figure 4B shows, the phenolate-type fluorescence at 425 nm is weakened, while the emission band of the phototautomer appears at 465 nm with stronger intensity. This behavior is similar to that observed for CD complexes and therefore indicates that the hydrophobic pockets of these hosts have sequestered HPMO. Now the blue emission of the dye provides information on the size of the hydrophobic cavity.

To obtain information on the size and flexibility of the caging cavity, we measured the fluorescence lifetime  $\tau$  and steady-state anisotropy  $\langle r \rangle$  of the phototautomers (**2** or **3**). They proved to be environment-dependent. In the micelle cage:  $\tau = 2.5$  ns [fitting to a biexponential function gives  $\tau_1 = 2.4$  (95%) and  $\tau_2 = 5.4$  ns (5%)] and  $\langle r \rangle = 0.035 \pm 0.006$ . When confined in  $\gamma$ -CD:  $\tau_1 = 2.1$  (24%),  $\tau_2 = 5.9$  ns (76%), and  $\langle r \rangle = 0.140 \pm 0.007$ . In calix[4]arene:  $\tau_1 = 0.8$  (88%),  $\tau_2 = 5.8$  ns (12%) and  $\langle r \rangle = 0.095 \pm 0.008$ . In the hydrophobic cavity of HSA:  $\tau_1 = 1.8$  (39%),  $\tau_2 = 5.7$  ns (61%), and  $\langle r \rangle = 0.245 \pm 0.003$ . Because both lifetime values change with the nature of the host, we cannot assign them to a specific fluorophore. However, we observe that the percentage

contribution of the longer time constant of the biexponential decay increases with increasing  $\langle r \rangle$ . The multiexponential decay of the emission can be explained by the existence of several twisted conformers of the probe with different angles between the aromatic moieties that are involved in the internal hydrogen bond and the subsequent proton transfer. Moreover, the motion of these moieties before and after the transfer can lead to different twisted fluorophores of the tautomer.

The amplitude of these motions is governed by the diameter of the cavity. Therefore, the structural changes are limited to a few species.

Since the hydrophobic core of the glucopyranoside micelles is formed by flexible alkyl chains and allows almost free twisting around the C2-C1' bond and possibly rotation of the caged phototautomer, the  $\langle r \rangle$  value is very low (0.035). However, in the case of calix[4]arene, the relatively high anisotropy (0.095) suggests some hindrance of these motions. Comparison with the anisotropy in CDs predicts an internal diameter of about 8 Å for the aromatic cavity of the host sequestering HPMO. This value is close to the average distance (ca. 7 Å) between face-to-face aromatic walls of calix[4]arene.<sup>[21]</sup>

The large anisotropy (0.245) of HPMO in HSA protein is remarkable. Because of the longer correlation rotational time of HSA in water (ca. 42 ns)<sup>[22]</sup> compared to the mean emission lifetime of sequestered HPMO (ca. 4.2 ns), we conclude that rotational motion of the protein does not influence the anisotropy of the probe. Hence, the high value of  $\langle r \rangle$  suggests that little reorientation of the fluorophore occurs during the lifetime of the excited state, and the direction of absorption and emission transition moments are not very different. In rigid films of poly(methyl methacrylate), where reorientation of the fluorophore is prevented, the steady-state anisotropy is  $0.325 \pm 0.005$ . In contrast, in fluid media such as dioxane, 3-methylpentane, and triacetin, we recorded zero anisotropy. The value of  $\langle r \rangle$  in HSA suggests that the dye is located in an environment with a cavity diameter smaller than that of  $\beta$ -CD (ca. 7.8 Å). On the basis of this and the X-ray structure of HSA,<sup>[23]</sup> the probe might be buried in the helical regions which form elongated pockets in the subdomains II and/or III of HSA (Scheme 1B), as was found for the binding of several ligands to this protein.<sup>[23]</sup>

Finally, we note that encapsulated HPMO is not expected to change the size and/or shape of CD and calix[4]arene. However, size and/or shape of micelles and HSA might be influenced by the presence of the guest. The above results suggest further experiments including time-resolved emission anisotropy measurements and consideration of the correlation rotational time of the host to obtain precise information on the molecular motion of the buried probe. Work in this direction is in progress in this group.

## Conclusion

We have shown that changes in the spectroscopic properties (position of absorption and steady-state emission and anisotropy) of a caged molecule (HPMO) can be used as a simple and powerful mean for exploring the size and hydrophobicity of nanocavities. These cavities range from spheres (micelles), cones and boxes (CDs and calixarenes) to more complex three-dimensional networks of channels (proteins) in supramolecular chemistry and molecular biology. Our results provide the basis for new ways for exploring molecular interactions and aid in the design of simple and efficient tools for the development of molecular science.

## Experimental Section

The sample of 2-(2'-hydroxyphenyl)-4-methyloxazole (HPMO) was obtained as previously described.<sup>[15]</sup> It was then purified by column chromatography, repeated crystallization from water/ethanol, and vacuum sublimation. The final sample consisted of white crystals. The purity was checked by HPLC; no evidence for impurities was found.  $\alpha$ -,  $\beta$ -, and  $\gamma$ -CD (Across Organics), *n*-octyl- $\beta$ -D-glucopyranoside (Across Organics, 98%), *cyclo*-undecylcalix[4]resorcinarene (Aldrich, 99%), human serum albumin (Sigma-Aldrich, 99%), and solvents (Aldrich, spectroscopy grade) were used as received. All experiments were performed with air-equilibrated fresh solutions.

UV/Vis absorption spectra were recorded on a Varian (Cary E1) spectrophotometer. Steady-state emission spectra and anisotropy [ $\langle r \rangle = (I_{\parallel} - GI_{\perp}) / (I_{\parallel} + GI_{\perp})$ ], where  $G$  is the correction factor for polarization responsivity of the apparatus,  $I_{\parallel}$  and  $I_{\perp}$  are the vertically and horizontally polarized emission intensities parallel and perpendicular to the plane of excitation, respectively] measurements were carried out with a Perkin-Elmer (LS-50B) spectrophotometer. Fluorescence lifetimes were measured by a time-correlated single-photon counting technique with a nanosecond fluorimeter (Edinburg Instruments, FL-900) equipped with a flash lamp fitted with hydrogen (pulse width ca. 800 ps). The time resolution of the apparatus is about 200 ps. The excitation wavelength was 320 nm. Fluorescence decays were analyzed by the method of nonlinear least-squares iterative deconvolution, and the quality of the fits was judged by the value of the reduced  $\chi_2$  and the autocorrelation function of the residuals. Details of the apparatus and data-analysis procedure have been published.<sup>[24]</sup> All absorption and emission measurements were performed at 298 K. <sup>1</sup>H NMR spectra of  $10^{-3}$  M solutions of HPMO in D<sub>2</sub>O in the absence and presence of  $10^{-2}$  M  $\beta$ -CD (almost saturated solution) were recorded at 500 MHz on a Varian Unity spectrometer at 303 K (reference: HDO at  $\delta = 4.62$ ).

The inclusion complexes were prepared by adding the appropriate amount of the host to an aqueous solution of HPMO. The mixture was then stirred until the host had completely dissolved.

## Acknowledgments

This work was supported by the Universidad de Castilla-La Mancha and DGICYT of Spain through project PB93-0126. I.G.O. thanks the Comunidad de Castilla-La Mancha for a doctoral fellowship.

- [1] a) A. H. Zewail, *Femtochemistry Ultrafast Dynamics of the Chemical Bond*, World Scientific, Singapore, **1994**; b) N. J. Turro, M. Grätzel, A. M. Braun, *Angew. Chem.* **1980**, *92*, 712; *Angew. Chem. Int. Ed. Engl.* **1980**, *19*, 675–696.
- [2] a) K. N. Houk, K. Nakamura, C. Sheu, A. E. Keating, *Science* **1996**, *273*, 627–629; b) D. Whang, J. Heo, J. H. Park, K. Kim, *Angew. Chem.* **1998**, *110*, 83–85; *Angew. Chem. Int. Ed.* **1998**, *37*, 78–80.
- [3] a) D. J. Cram, M. E. Tanner, R. Thomas, *Angew. Chem.* **1991**, *103*, 1048–1051; *Angew. Chem. Int. Ed. Engl.* **1991**, *30*, 1024–1027; b) F. Pina, A. J. Parola, E. Ferreira, M. Maestri, N. Armadori, R. Ballardini, V. Balzani, *J. Phys. Chem.* **1995**, *99*, 12701–12703; c) W. Herrmann, M. Schneider, G. Wenz, *Angew. Chem.* **1997**, *109*, 2618–2621; *Angew. Chem. Int. Ed. Engl.* **1997**, *36*, 2511–2514.
- [4] a) V. Balzani, F. Scandola, *Supramolecular Photochemistry*, Ellis Horwood, London, **1991**; b) V. Ramamurthy, *Photochemistry in Organized and Constrained Media* (Ed.: V. Ramamurthy), VCH, Cambridge, **1991**; c) J.-M. Lehn, *Supramolecular Chemistry: Concepts and Perspectives*, VCH, Weinheim, **1995**.
- [5] a) P. Timmerman, W. Verboom, F. C. J. M. van Veggel, J. P. M. van Duynhoven, D. N. Reinhoudt, *Angew. Chem.* **1994**, *106*, 2437–2441; *Angew. Chem. Int. Ed. Engl.* **1994**, *33*, 2345–2348.
- [6] G. Wenz, *Angew. Chem.* **1994**, *106*, 851; *Angew. Chem. Int. Ed. Engl.* **1994**, *33*, 803–822.
- [7] D. B. Amabilino, J. F. Stoddart, *Chem. Rev.* **1995**, *95*, 2725–2828.
- [8] P. Bortolus, S. Monti, *Adv. Photochem.* **1996**, *21*, 1–133.
- [9] D. Philp, J. F. Stoddart, *Angew. Chem.* **1996**, *108*, 1242–1286; *Angew. Chem. Int. Ed. Engl.* **1996**, *35*, 1154–1196.
- [10] L. Jullien, J. Canceill, B. Valeur, E. Bardez, J.-M. Lehn, *Angew. Chem.* **1994**, *106*, 2582–2584; *Angew. Chem. Int. Ed. Engl.* **1994**, *33*, 2438–2439.
- [11] S. Vajda, R. Jimenez, S. J. Rosenthal, V. Fidler, G. R. Fleming, E. W. Castner, *J. Chem. Soc. Faraday Trans.* **1995**, *91*, 867–873.
- [12] a) A. Douhal, F. Amat-Guerri, A. U. Acuña, *Angew. Chem.* **1997**, *109*, 1586–1588; *Angew. Chem. Int. Ed. Engl.* **1997**, *36*, 1514–1516; b) A. Douhal, *Ber. Bunsenges. Phys. Chem.* **1998**, *102*, 448–451.
- [13] A. Douhal, T. Fiebig, M. Chachisvilllis, A. H. Zewail, *J. Phys. Chem. A* **1998**, *102*, 1657–1660.
- [14] C. R. Mateo, A. Douhal, *Proc. Natl. Acad. Sci. USA* **1998**, *95*, 7245–7250.
- [15] V. Guallar, M. Moreno, J.-M. Lluch, F. Amat-Guerri, A. Douhal, *J. Phys. Chem.* **1996**, *100*, 19789–19794.
- [16] a) A. Douhal, S. Kim, A. H. Zewail, *Nature* **1995**, *378*, 260–263; b) M. Chachisvilllis, T. Fiebig, A. Douhal, A. H. Zewail, *J. Phys. Chem. A* **1998**, *102*, 669–673.
- [17] A. Douhal, F. Lahmani, A. H. Zewail, *Chem. Phys.* **1996**, *207*, 477–498.
- [18] A. Douhal, *Science* **1997**, *276*, 221–222.
- [19] C. Chudoba, E. Riedle, M. Pfeiffer, T. Elsaesser, *Chem. Phys. Lett.* **1996**, *263*, 622–628.
- [20] A. Douhal, F. Lahmani, A. Zehnacker-Rentien, F. Amat-Guerri, *J. Phys. Chem.* **1994**, *98*, 12198–12205.
- [21] K. B. Lipkowitz, G. Pearl, *J. Org. Chem.* **1993**, *58*, 6729–6736.
- [22] C. R. Mateo, personal communication.
- [23] X. Min He, D. C. Carter, *Nature* **1992**, *358*, 209–215.
- [24] D. Reyman, M. H. Viñas, J. M. L. Poyato, A. Pardo, *J. Phys. Chem. A* **1997**, *101*, 768–775.

Received: July 13, 1998

Revised version: September 21, 1998 [F1258]